17th World Conference on Earthquake Engineering, 17WCEE
Sendai, Japan - September 13th to 18th 2020

DAMAGE DETECTION IN STRUCTURES USING RESPONSE SIGNAL DECOMPOSITION THROUGH WAVELETS

M.B. Waris[1], H. Ibrahim[2], K.M. Abu-Sohel[3], M. A. El-Gelil[4]

[1] *Assistant Professor, Dept. of Civil and Architectural Engineering, Sultan Qaboos University, Oman, waris@squ.edu.om*
[2] *Graduate Student, Dept. of Civil and Architectural Engineering, Sultan Qaboos University, Oman, s117893@student.squ.edu.om*
[3] *Assistant Professor, Dept. of Civil and Architectural Engineering, Sultan Qaboos University, Oman, kmasohel@squ.edu.om*
[4] *Assistant Professor, Dept. of Civil and Architectural Engineering, Sultan Qaboos University, Oman, mahmouda@squ.edu.om*

Abstract

Monitoring the response of structures during catastrophic events is essential for structural health monitoring and damage detection. Using this response, vibration-based damage detection techniques can isolate the change in dynamic characteristics of the structure to identify the occurrence of damage. This study uses numerical modeling to present an approach based on discrete wavelet analysis for damage detection in structures, through comparison of the ground acceleration with the structural response. The proposed method is verified using the structural response under six different earthquake excitations, namely Kobe (1995), Athens (1999), Imperial Valley (1979), Loma Prieta (1989), Cape Mendocino (1992) and Chuetsu-oki (2007). Two-dimensional single-story steel frames having one and two bay are subjected to scaled earthquake histories to cause damage that does not exceed the Immediate Occupancy (IO) Limit. The structural models accounted for second-order effects and considered the nonlinear behavior through plastic hinges at the ends of each element based on ASCE41-13. The response was calculated using nonlinear direct integration time history analysis and damage was considered as the initiation of plastic rotation in the hinges. The method was able to detect the time of occurrence of damage in all cases. It also provided good information about the general location of damage. The ability to detect damage was observed to be more sensitive to the natural period of the structures rather than the average period of the earthquake.

Keywords: Damage Detection, Wavelet Transform, Plastic Damage, Earthquake.

1 Introduction

Damage detection has prime importance for the assessment of structural integrity, followed by repair and maintenance. In general, damage detection aims to determine the presence and location of damage, quantify its severity, and finally estimate the remaining service life of the structure [1]. Damage can be localized by visual inspection; however, structural elements in buildings are usually concealed by architectural finishing, which makes the visual inspection impossible. Structural Health Monitoring (SHM) represents an efficient way to monitor the performance of the structure and evaluate its condition by the use of sensors. SHM can permit the early detection of any damage, even before it becomes visible, and thus improves the safety of the building, protecting lives and reducing maintenance costs. Most SHM techniques use modal analysis methods for the localization of damage. The premise of these methods is that the modal parameters are function of the mechanical properties of the structure. One of the popular methods in structural damage detection is the identification of the changes in modal characteristics by comparing the damaged and undamaged states of the structure [2]. Unfortunately, the undamaged response is not always available. Moreover, experiments show that in large structures, modal characteristics might be insensitive to localized damage [3]. In addition, due to signal corruption by noise, changes in mode shapes might be unidentifiable [4]. Since modal analysis is performed in the frequency domain, high resolution in frequency and time cannot be obtained simultaneously. Wavelet Analysis is a technique that allows the use of long time intervals for low-frequency information, and short time intervals for high-frequency information, which has led to its recent widespread application in many fields of engineering [4].

Much research [2, 4-12] has been done on the use of Continues Wavelet Transform (CWT) and Discrete Wavelet Transform (DWT) in structural health monitoring. However, DWT is considered more suitable to detect the time of change in frequency due to stiffness degradation in a structure [11]. In most of these studies, simple structures like beams and simple frames were considered and damage was introduced in the structure, resulting in a sudden change in stiffness at the location. Such damage would lead to large deformations that might be detected by visual inspection. When a structure is subjected to earthquakes, if the excitation is small, the structure will behave elastically, and thus the structure will remain undamaged. On the other hand, when the excitation is strong enough to cause considerable deformations and push the structure beyond the elastic range, damage will be obvious and detectable by visual inspection. Between these two scenarios, a structure may exceed the elastic range with small plastic rotations. The SHM approach should be able to capture such small damage and should be verified for the seismic excitation of different characteristics. Except for Vaez and Aghdaei [12], all the studies used only one ground motion record, when considering earthquake excitation. This study, therefore, is an attempt to investigate the ability of the wavelet transform to detect the occurrence of minor plastic damage in structures and to verify the performance using different earthquake histories. Two-dimensional steel frames with one and two bays are modeled in ETABS 2016 [13] and subjected to six earthquakes excitations that are individually scaled to develop plastic hinges in the frames.

2 Modeling

2.1 Modeling Damage

The damage in the frame was simulated through plastic hinges and all plastic deformations were assumed to occur within the hinges. The hinge properties were modeled as per ASCE 41-13 [14] and the nonlinear behavior under monotonic loading was defined by the well-known bilinear hysteretic model shown in Fig. 1. The curve has five distinct points:

- Point A is the origin: no applied load and no deformation.
- Point B is the yield point.
- Point C represents the point of ultimate capacity.
- Point D represents the residual resistance.
- Point E represents the total failure.

Before reaching point B, deformations are linear and take place within the element itself without plastic deformations in the hinge. The hinge unloads elastically along slope AB without any plastic deformation. After

exceeding point B, the hinge will unload with the initial stiffness as in the elastic stage, i.e. parallel to AB. Points IO (immediate occupancy), LS (life safety), and CP (collapse prevention) are indicative thresholds used in performance-based design. The goal of this research was to target the plastic behavior of the structure that does not exceed the IO state of the hinge.

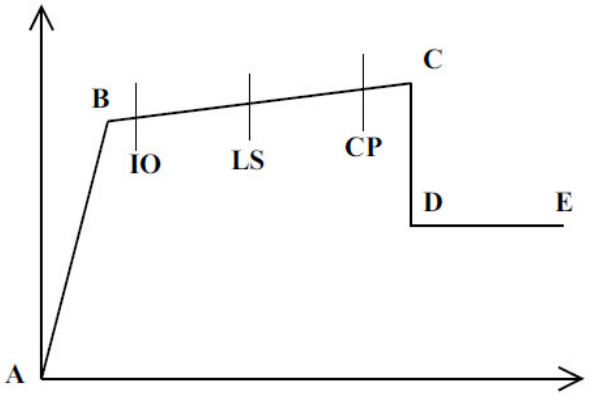

Fig. 1 Bilinear Load-Deformation Model [15]

2.2 Earthquake Histories

To account for the characteristics of different earthquakes, six ground motion histories were considered in this study:

- Kobe (Japan) earthquake of 16 January 1995, recorded by Kakogawa (CUE90) station.
- Athens (Greece) earthquake of 7 September 1999, recorded by Athens-Syntagma station.
- The Imperial Valley (USA) earthquake of 15 October 1979, recorded by USGS station 5115.
- Loma Prieta (USA) earthquake of 17 October 1989, recorded by station Anderson Dam (L Abut).
- Cape Mendocino (USA) earthquake of 25 April 1992, recorded by Loleta Fire station.
- Chuetsu-oki (Japan) earthquake of 16 July 2007, recorded by Joetsu Ogataku station.

The 5% damped response spectra of the original earthquakes for a are shown in Fig. 2, indicating the difference in their characteristics. The earthquake histories were used with different scaling factors to cause damage to the frames used in this study.

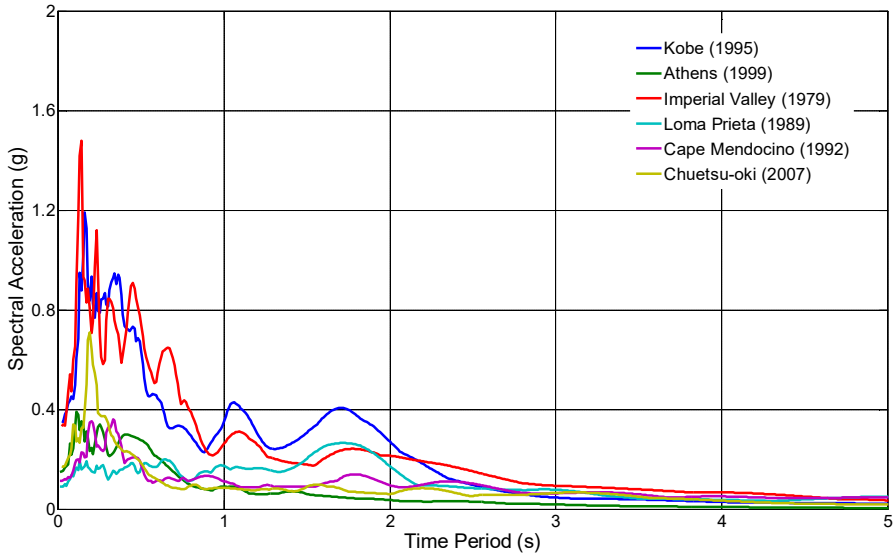

Fig. 2 Response Spectrum of the Selected Earthquakes

2.3 Numerical Modelling

Fig. 3 shows the one- and two-bay steel frame used in this research. The frames were 3.0 m high, and the beam span was also 3.0 m. All columns were assumed to be fixed at the base. All elements were made of S355 steel having a modulus of elasticity E=210 GPa, shear modulus G=81 GPa. All beams were HEA 160 and all columns section were HEB 160. The sections were selected to ensure strong column-weak beam behavior. The columns, beams and joints are labeled as indicated in the figure to facilitate discussion of results in section 3. The self-weight of the frame elements was calculated using a unit weight of 77 kN/m^3 and an additional imposed load of 40kN/m was considered on the beams. ETABS [13] was used to model the frames and the dynamic analysis was carried out using nonlinear direct-integration time history analysis with a time-step of 0.01 sec time step using the Newmark method (γ=0.5 β=0.25). The natural period of the two frames shown in Fig. 3(a) and (b) were estimated as 0.43 sec and 0.48 sec respectively.

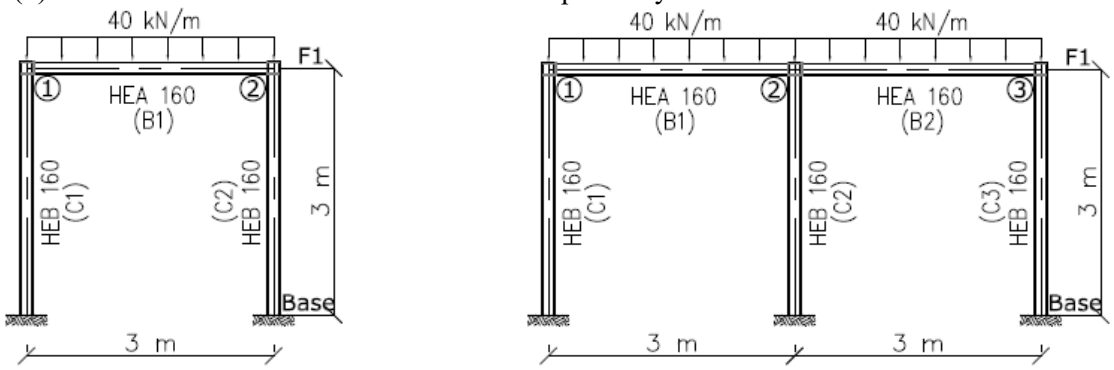

(a) One-bay frame (b) Two-bay frame

Fig. 3 Schematic of the two steel frames used in the study

2.4 Response Signal Processing

Since the ground motion due to the earthquake may contain changes in frequency, these changes will cause spikes in the wavelet details of the input signal [11]. Moreover, these frequency pulses propagate through the structure, and will also appear as spikes in the wavelet details of the response signals at all stories [6]. To deal with this issue, the current research suggests that the input signal should be analyzed by DWT to identify the spikes observed in detail due to frequency shifts of ground motion. The spikes remaining after the comparison will represent occurrence of damage due to changes in structural characteristics. Therefore, in this research, the correlation between the input and output signals was used. The correlation was based on the fact that the total acceleration $\ddot{u}_n^T(t)$ at floor $'n'$ of a structure subjected to an earthquake ground acceleration, $\ddot{u}_g(t)$, is given by Eq. (1):

$$\ddot{u}_n^T(t) = \ddot{u}_g(t) + \ddot{u}_n(t) \tag{1}$$

where $\ddot{u}_n(t)$ is the acceleration at floor $'n'$ relative to the ground. Hence, the equation of motion for a structure subjected to earthquake ground acceleration $\ddot{u}_g(t)$ is given by Eq. (2).

$$m\ddot{u}(t) + c\dot{u}(t) + ku(t) = -m\ddot{u}_g(t) \tag{2}$$

where $u(t)$ is the displacement vector, $\dot{u}(t)$ is the velocity vector, $\ddot{u}(t)$ is the acceleration vector, m is the mass matrix, c is the damping matrix, and k is the stiffness matrix. The acceleration response of all the joint under the earthquake excitation was analyzed by the discrete wavelet analysis upto the fifth level of decomposition with the biorthogonal (bior6.8) wavelets presented in Fig. 4. Signal Decomposition was done using MATLAB and details were plotted to examine for spikes. Usually, the first level detail signal is sufficient to identify the discontinuities due to damages in signals without noise [5,11]. The presence of spikes in the detail indicated damage and the time at which the spike appeared represents the time of occurrence of damage.

If no spikes were observed in the detail signal, it meant the structural behavior is still elastic and no damage has occurred.

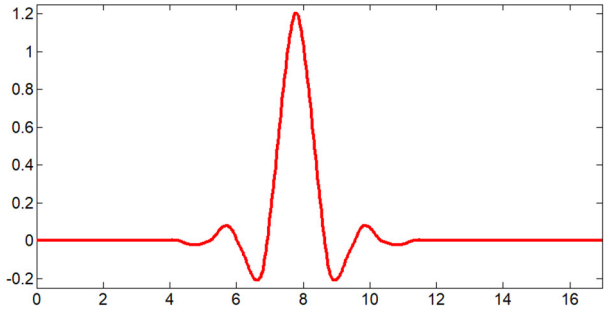

Fig. 4 The bi-orthogonal (bior6.8) wavelet used in the study

3 Results and Discussion

As mentioned earlier, the study considered six different earthquake histories to investigate the performance of the method to detect damage in the two frames. It was observed that the approach was able to accurately identify the occurrence of damage in the case of all the earthquakes in the two frames. The two subsequent sections (3.1 and 3.2) discuss the procedure used for damage detection in the study for one bay and two bay frames for the Kobe (1995) earthquake. A summary of all the earthquakes is discussed in section 3.3.

3.1 Single Bay Frame

The one-bay frame in Fig. 3(a), when subjected to the original Kobe Earthquake excitation, did not develop any plastic hinges and the frame remained elastic. The input was scaled up gradually and the nonlinear time history analysis was performed until plastic hinges developed. At a scale factor of 2.0, three plastic hinges were developed between $t_1 = 7.4\ sec$ and $t_2 = 7.42\ sec$ as indicated in the Fig. 5(a). The moment-rotation curves of the plastic hinges at the three locations are presented in Fig. 5(b)-(d), as extracted from ETABS. As can be observed that H1 and H2 have yielded but the plastic rotation is below the limit for immediate occupancy (IO), indicated in the respective figures. The plastic rotation at H1 and H2 were recorded as $4.39 \times 10^{-3}\ rad$ and $1.65 \times 10^{-3}\ rad$ respectively. The plastic rotation at H3 was $5.31 \times 10^{-3}\ rad$ that exceeded the IO limit for the beam.

The input ground motion and response acceleration signal at joint-1 and joint-2 were analyzed using DWT and the first level detail signals are given in Fig. 6. The detail of the input and output appear very similar and no information about damage can be concluded. This is due to the fact that the frequency content of the earthquake excitation will propagate through the structure and appear as spikes in the details of the response signals. As per the proposed methodology, the detail on input signal (earthquake) and output (joint acceleration) were added and the resulting signal is given in Fig. 7. It shall be noted that the correlation of the input and output signals was calculated and the time lag was found to be zero. The spike due to the formation of plastic hinge is evident from the figure. The time of appearance of the spike at $t_1 = 7.4\ sec$ is the same as the time of hinge formation. The plastic hinges (H1, H2, and H3) in the columns and beam occurred over a short interval ($t_1 = 7.4\ sec$ and $t_2 = 7.42\ sec$), which explains why spikes were observed in that narrow interval. Although the plastic rotations were small, DWT coupled with the proposed technique was able to capture the damage as spikes in the detail.

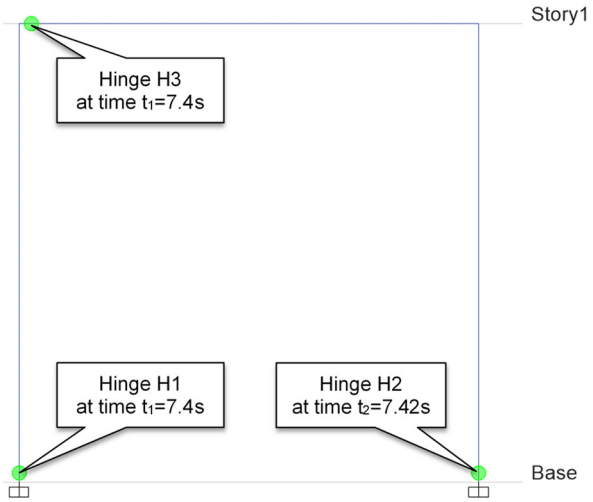

(a) Location of Plastic Hinges

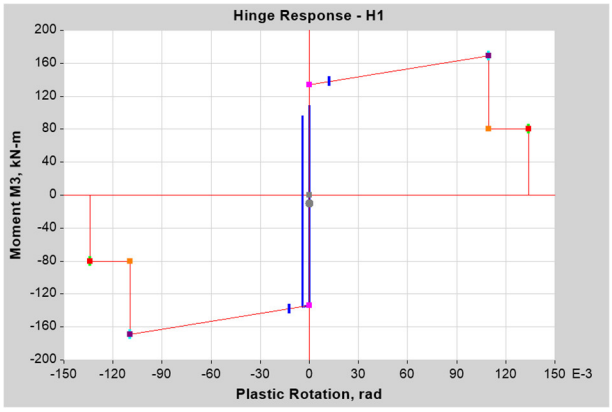

(b) Hinge H1 at base of C1

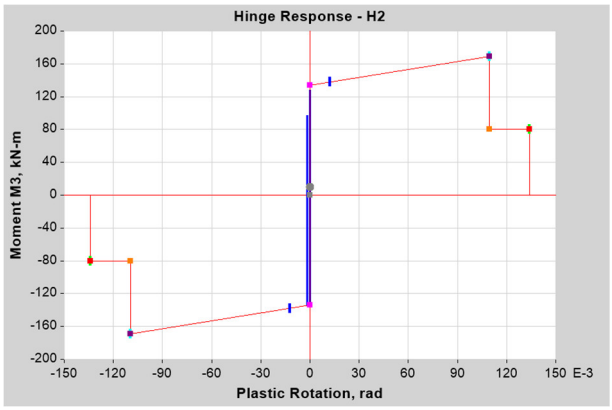

(c) Hinge H2 at base of C2

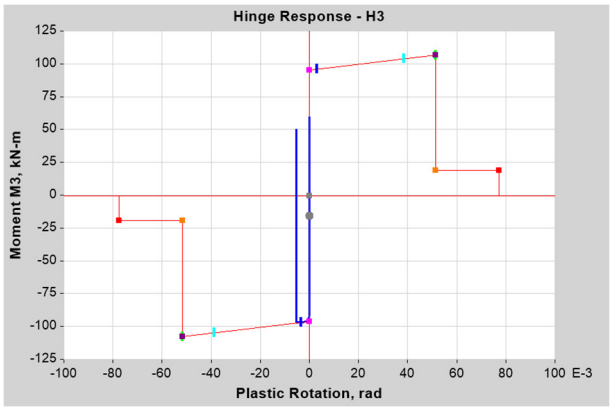

(d) Hinge H3 at the left end of B1

Fig. 5 Formation of plastic hinges in one-bay frame subjected to the Kobe earthquake (S.F=2)

It is noteworthy that the maximum signal amplitude at Joint-1 (magnitude of the spike) was 116.8 mm/s^2, which is greater than the value at Joint-2, which was 81.40 mm/s^2. The moment-rotation diagrams in Fig. 5 show that the hinges H1 and H3 that are close to Joint-1, underwent larger plastic rotation compared to H2 that is close to Joint-2. This indicates that it might be possible to identify the region with greater damage based on the amplitude of spike using signals from different locations.

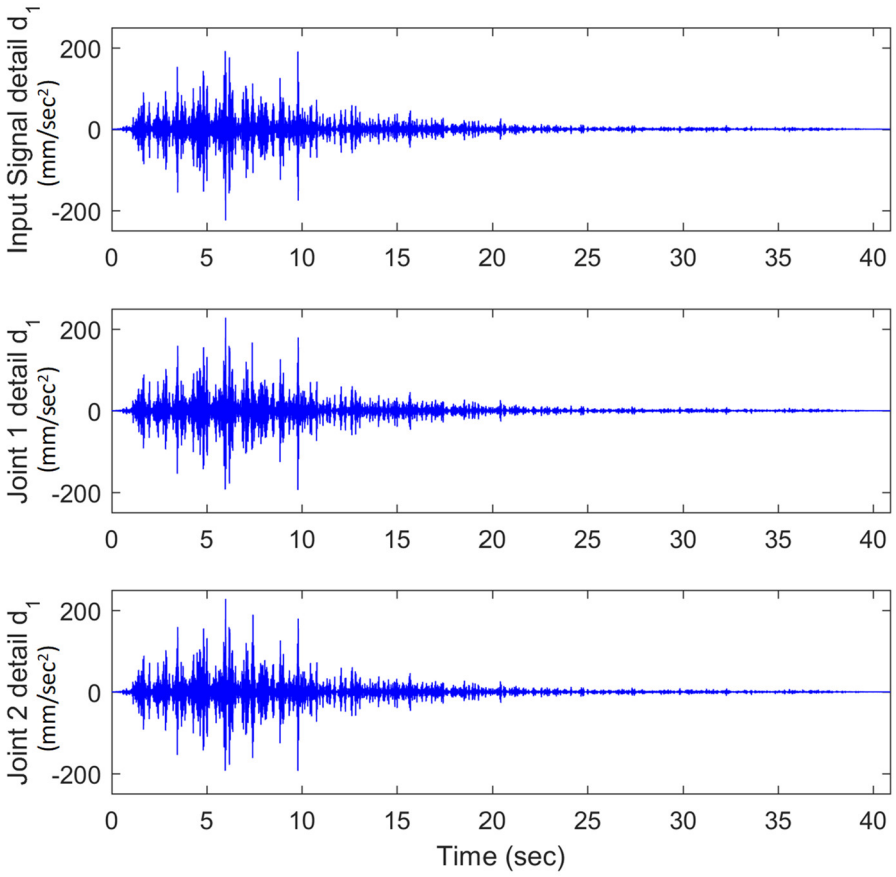

Fig. 6 Details of the one-bay frame subjected to Kobe earthquake (S.F=2.0)

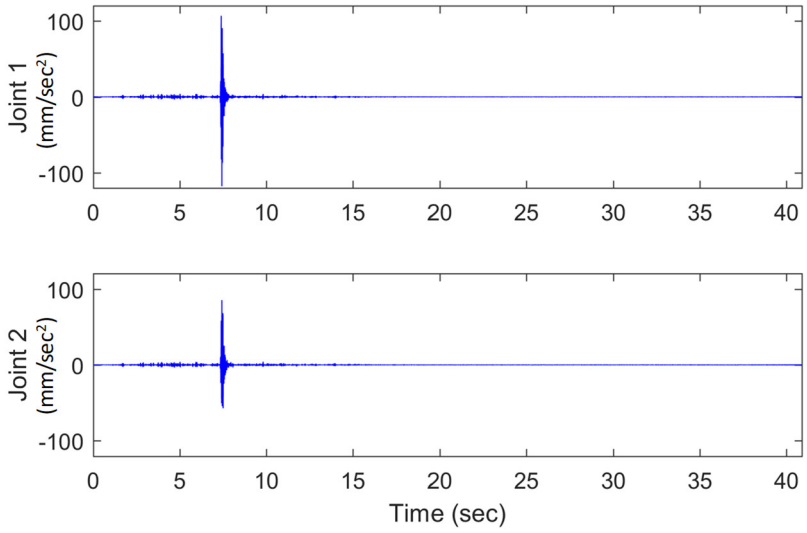

Fig. 7 Damage detection in the one-bay frame subjected to the Kobe earthquake (S.F=2.0)

Since the plastic rotation in the previous case exceeded IO state, the scale factor of the Kobe earthquake was set to 1.65, to reduce the damage. Under the excitation, only one plastic hinge appeared at time $t_1 = 7.43\ sec$ at the base of column C1, as shown in Fig. 8 (a). The maximum plastic rotation of hinge H1 was

$2.85 \times 10^{-4}\ rad$. Although the plastic rotation is very small as visible in Fig. 8 (b), the proposed method is able to indicate a spike that appeared at the time of the hinge formation. Again the amplitude of spike at Joint-1, just above the hinge was 17.20 mm/s^2, which is greater than the farther Joint-2, which was 12.70 mm/s^2. The results, therefore, indicate that the closer the damage, the higher will be the spike amplitude. Moreover, the method is sensitive to the level of damage, i.e. more severe damages yield greater coefficients, and consequently larger spikes as the spike amplitude was an order different similar to the plastic rotation.

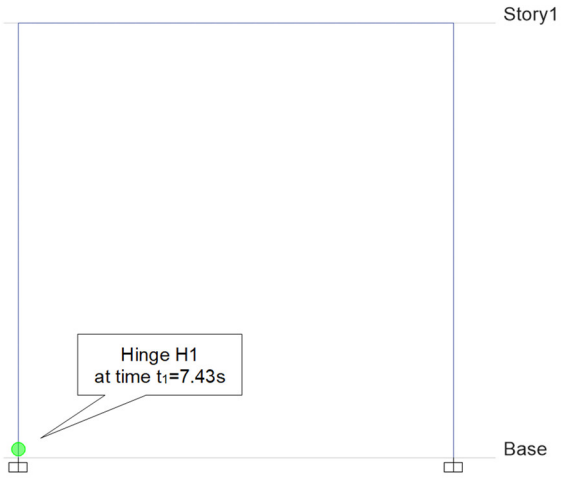

(a) Location of Plastic Hinge

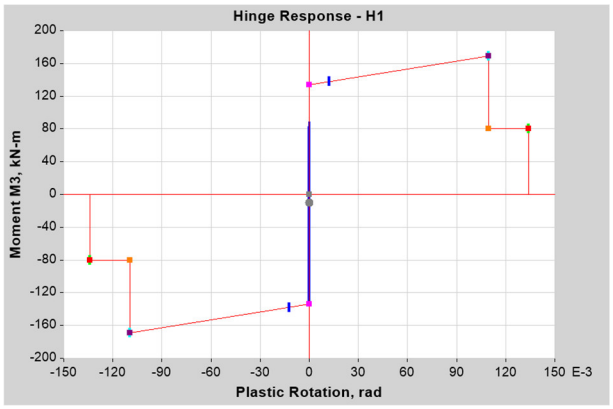

(b) Moment-Rotation Diagram

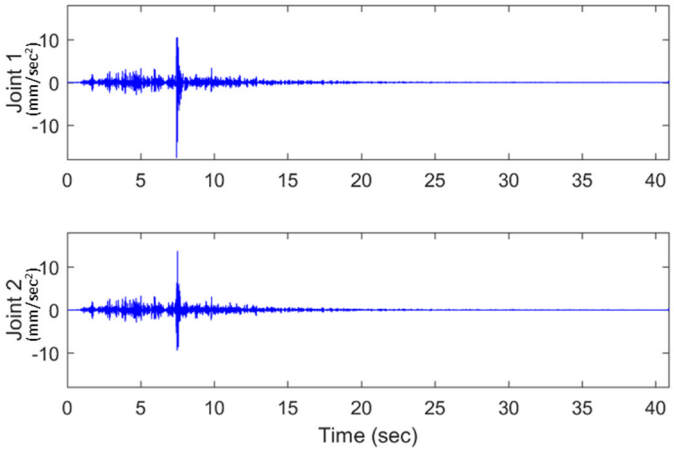

(c) Detail of acceleration signal at joints

Fig. 8 Formation of plastic hinges in the one-bay frame subjected to the Kobe earthquake (S.F=1.65)

3.2 Two Bay Frame

The two-bay frame in Fig. 3(b) was subjected to the Kobe earthquake using a scale factor of 1.35 and a plastic hinge formed on the base of column C2 at $t_1 = 5.65\ sec$ as indicated in Fig. 9(a). The results from the dynamic analysis showed that the plastic hinge was formed with a rotation of $8.43 \times 10^{-4}\ rad$ as indicated in Fig. 9(b). The input earthquake acceleration and output joint accelerations were analyzed with DWT using the approach discussed earlier and the resulting details for Joint-1, Joint-2 and Joint-3 are presented in Fig. 9(c). The figure clearly shows a spike in the signal detail of the three joints at the instant when the plastic hinge was formed. It is noted that the magnitudes of the spikes were 15.3 mm/s^2, 24.24 mm/s^2 and 15.63 mm/s^2 at Joint-1, Joint-2, and Joint-3, respectively. The largest spike at Joint-2, which is nearest to the plastic hinge (damage), while Joint-1 and Joint-3 almost have similar spike magnitude as they lie at the same distance from the location

of the damage. This further reinforces the observation made in case of the one-bay frame regarding possible relationship between the amplitude of spike and proximity to damage.

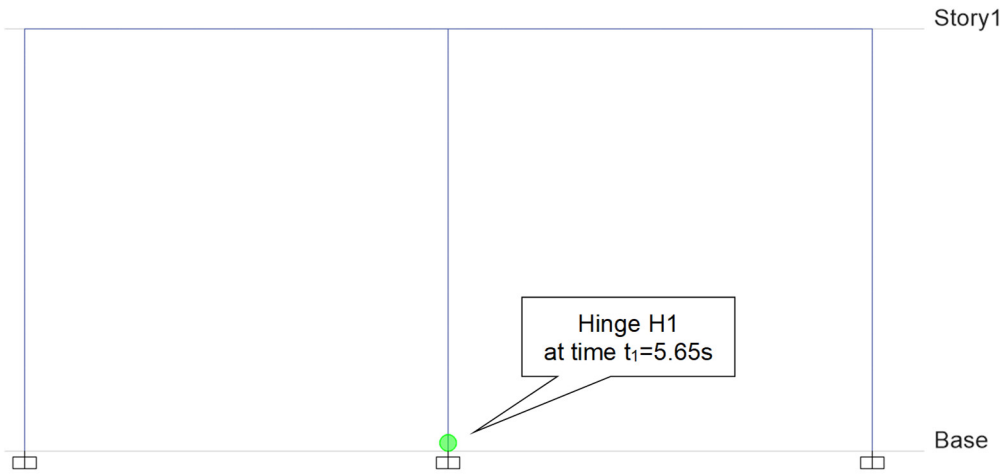

(a) Plastic hinge location

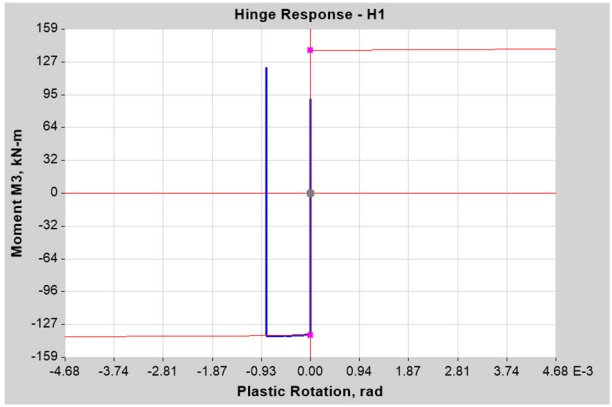

(b) Moment-Rotation Diagram

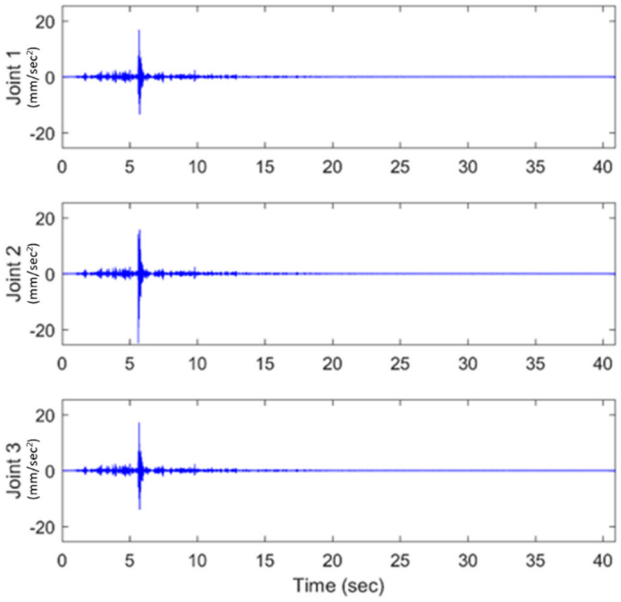

(c) Detail of processed signal at respective joint

Fig. 9 Damage detection in the two-bay frame subjected to the Kobe earthquake (S.F= 1.35)

3.3 Summary of Results

Finally, to study the influence of different earthquake histories, five other earthquakes mentioned previously were considered and the scaling factor was estimated using trial and error to induce damage in the frame. Care was exercised that the plastic rotation is small, therefore, only a single plastic hinge was observed in all cases. A summary of the parameters from each case is provided in Table 1. For the one-bay frame, the damage varied between $1.61 \times 10^{-4} - 4.05 \times 10^{-4} rad$ with the time of formation of plastic hinge varied between $6.96 - 20.15\ sec$, while for the two-bay frame the damage varied between $2.04 \times 10^{-4} - 9.62 \times 10^{-4} rad$ with the time of hinge formation varying between $5.65 - 20.15\ sec$. The proposed method was able to detect damage in ALL case, with spike appearing at the same time as observed in the simulation.

Fig. 10 shows a comparison of the magnitude of plastic rotation and the maximum amplitude of spike observed in the respective case. The bar graph represents the plastic rotation while the spike ampltide is presented using lines. The amplitude of the spike is very clearly sensitive to the magnitude of plastic rotation in the respective frames and the relationship is nearly linear for both the frames. The maximum spike amplitude is smaller in case of the two-bay frame, even with higher plastic rotations, therefore, it can be concluded that as the structure becomes more complex, the spike amplitude is attenuated.

Table 1: Summary of Damage Detection for all Earthquakes

Earthquake		**Kobe (1995)**	**Athens (1999)**	**Loma Prieta (1989)**	**Cape Mendocino (1992)**	**Chuetsu-Oki (2007)**	**Imperial Valley (1979)**
Mean Period [16]		0.542	0.449	1.246	0.808	0.562	0.494
1-Bay Frame	Scale Factor	1.65	3.95	6.6	5.9	5.2	1.38
	Time (s)	7.43	9.08	6.96	8.8	20.15	11.35
	Pl. Rot. ($x10^{-4}$ rad)	2.85	1.61	4.05	`2.65	3.2	2.39
	Hinge Location	Base of C1	Base of C2	Base of C2	Base of C1	Base of C1	Base of C1
2-Bay Frame	Scale Factor	1.35	3.15	6.3	4.5	4.85	1.14
	Time (s)	5.65	9.14	6.99	9.09	20.15	11.42
	Pl. Rot. ($x10^{-4}$ rad)	8.43	2.05	7.12	9.62	2.04	8.59
	Hinge Location	Base of C2	Base of C2	Base of C2	Base of C2	Base of C2	Base of C2

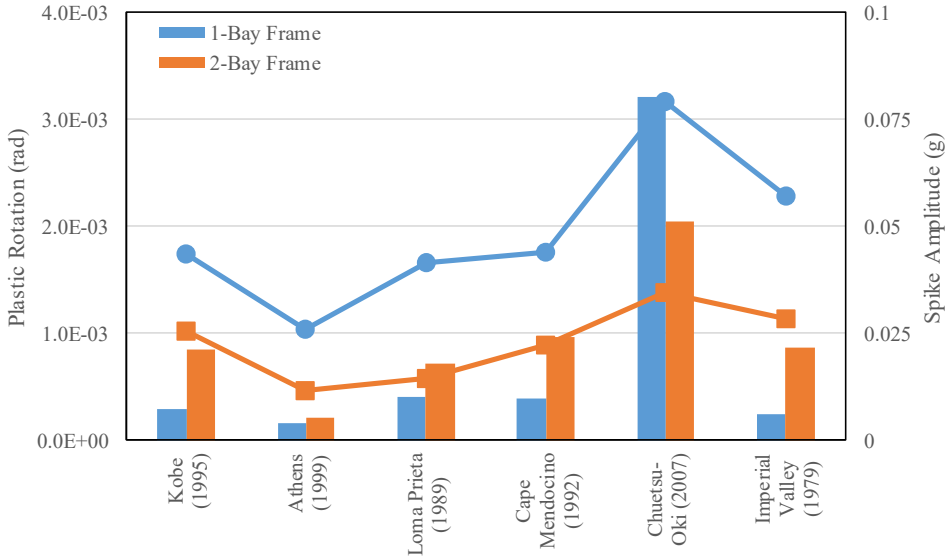

Fig. 10 Platic Rotation vs Spike amplitude for all the Earthquakes

In order to identify the influence of the frequency content of earthquake on damage detection, the mean period for each earthquake was calculated using Eq. (3) following Rathje et al [16].

$$T_m = \frac{\sum_i C_i^2 . \left(\frac{1}{f_i}\right)}{\sum_i C_i^2} \qquad for\ 0 \cdot 25Hz \leq f_i \leq 20Hz \tag{3}$$

where C_i denotes the Fourier amplitudes and f_i the frequencies of the Fourier transform. The calculated values are included in Table 1, which vary between $0.45 - 1.25\ sec$. The frames used in this study had natural periods of 0.45 sec and 0.48 sec and did not indicate any correlation with the mean period of the earthquake in terms of damage detection. However, the scaling factors were larger for earthquakes with the higher mean period (Loma Prieta, Caper Mendocino) and smaller otherwise. Further, for similar mean period, the scaling factor for strong earthquakes (Kobe, Imperial Valley) is much less than moderate earthquakes (Athens, Chuetsu-Oki). This indicates that damage detection is independent of the overall frequency content of the earthquake, while the development of damage is dependent on the energy transmitted by the earthquake excitation into the structure.

4 Conclusions

A damage detection technique based on discrete wavelet analysis was investigated using numerical modeling of one- and two-bay steel frames. Six different earthquake histories were used to investigate the performance of the approach. The technique was able to detect minor plastic rotation in all cases considered. It was found that the spike amplitude is sensitive to the magnitude of plastic rotation and distance to the location of the plastic hinge. The spike amplitude was found to be linearly related to damage (plastic rotation). It was observed that damage detection is not sensitive to the characteristics of an earthquake, however, the mean period of the earthquake was observed to be representative of the ability of an earthquake to cause damage in the structure.

5 References

[1] Rytter, A. (1993). Vibrational based inspection of civil engineering structures (Doctoral dissertation, Dept. of Building Technology and Structural Engineering, Aalborg University).

[2] Bagheri, A., & Kourehli, S. (2013). Damage detection of structures under earthquake excitation using discrete wavelet analysis, Asian Journal of Civil Engineering (BHRC), 14(2), 289-304.

[3] Friswell, M. I., & Penny, J. E. T. (1997, June). Is damage location using vibration measurements practical. In Euromech 365 international workshop: Damas (Vol. 97, pp. 351-362).

[4] Taha, M. R., Noureldin, A., Lucero, J. L., & Baca, T. J. (2006). Wavelet transform for structural health monitoring: a compendium of uses and features. Structural Health Monitoring, 5(3), 267-295.

[5] Ovanesova, A. V., & Suarez, L. E. (2004). Applications of wavelet transforms to damage detection in frame structures. Engineering structures, 26(1), 39-49.

[6] Todorovska, M. I., & Trifunac, M. D. (2005). Structural health monitoring by detection of abrupt changes in response using wavelets: application to a 6-story RC building damaged by an earthquake. In Proc. of the 37th Joint Panel Meeting on Wind and Seismic Effects (pp. 1-20).

[7] Bajaba, N. S., & Alnefaie, K. A. (2005). Multiple damage detection in structures using wavelet transforms. Emirates J. Eng. Res, 10, 35-40.

[8] Rucka, M. (2011). Damage detection in beams using wavelet transform on higher vibration modes. Journal of theoretical and applied mechanics, 49(2), 399-417.

[9] Patel, S. S., Chourasia, A. P., Panigrahi, S. K., Parashar, J., Parvez, N., & Kumar, M. (2016). Damage Identification of RC Structures Using Wavelet Transformation. Procedia Engineering, 144, 336-342.

[10] Janeliukstis, R., Rucevskis, S., Wesolowski, M., & Chate, A. (2017). Multiple damage identification in beam structure based on wavelet transform. Procedia Engineering, 172, 426-432.

[11] Pnevmatikos, N. G., & Hatzigeorgiou, G. D. (2017). Damage detection of framed structures subjected to earthquake excitation using discrete wavelet analysis. Bulletin of Earthquake Engineering, 15(1), 227-248.

[12] Vaez, S. R. H, & Aghdaei, S. S. T. (2018). Effect of the frequency content of earthquake excitation on damage detection in steel frames. Journal of Rehabilitation in Civil Engineering.

[13] ETABS 2016, Computer and Structures Inc, https://www.csiamerica.com/products/etabs.

[14] ASCE/SEI 41-13, 2013, Seismic Evaluation and Retrofit of Existing Buildings, American Society of Civil Engineers, Reston, VA.

[15] CSI Analysis Reference Manual. (2017). CSI Analysis Reference Manual for SAP2000®, ETABS®, SAFE® and CSiBridge®.

[16] Rathje, E. M., Abrahamson, N. A., & Bray, J. D. (1998). Simplified frequency content estimates of earthquake ground motions. Journal of Geotechnical and Geoenvironmental Engineering, 124(2), 150-159.

